Ordered Self-Assembling of Tetrahedral Oxide Nanocrystals

J. S. Yin and Z. L. Wang*

School of Materials Science and Engineering, Georgia Institute of Technology, Atlanta, Georgia 30332-0245

(Received 19 June 1997)

Self-assembling of size, shape, and phase controlled nanocrystals into superlattices with translational and even orientational ordering is a new approach for engineering nanocrystal materials and devices. High purity tetrahedral nanocrystals of CoO, with edge lengths of 4.4 ± 0.2 nm, were synthesized and separated from Co nanocrystals, using a novel magnetic field phase-selection technique. Self-assembling of the faceted CoO nanocrystals forms ordered superlattices, the structures of which are determined. [S0031-9007(97)04151-3]

PACS numbers: 81.05.Ys, 61.46.+w

Nanocrystal engineered materials are a new generation of materials that have attracted considerable interest in many fields [1–10]. Recent research has successfully fabricated *self-assembly passivated nanocrystal superlattices (NCS's) or nanocrystals arrays (NCA's)* of metal [11–16], semiconductor [17–19], oxide [20], and sulfite [21] clusters, which are a new form of materials with fundamental interests and potential technological applications. Naturally, the size and shape selected nanocrystals behave like ideal building blocks for two- and three-dimensional cluster self-assembled superlattice structures, in which the particles behave as well-defined "molecular matter" and they are arranged with long-range translation and even orientation order [22]. Well-defined ordered solids prepared from tailored nanocrystalline building blocks provide new opportunities for optimizing and enhancing the properties and performance of the materials. This is a new initiative of research on *cluster engineered materials.*

Self-assembled arrays involve self-organization into monolayers, thin films, and/or superlattices of size-selected nanoclusters encapsulated in protective compact organic coating. A key step in this process is the fabrication of size and shape controlled nanocrystals. Most of the current studies have been carried out for nanocrystals whose shape can be approximated as spherical; thus, they can be considered as large "atoms," forming superlattices with body-centered cubic, face-centered cubic, or hexagonal close-packed structure. The study of Ag NCS by Harfenist *et al.* [15] has, however, clearly shown the vital role played by particle shape on the packing crystallography of the superlattice. In this Letter, we report, for the first time, the success of preparing self-assembled NCS of CoO nanoclusters with a tetrahedral shape and monosize distribution. A particle selection technique using magnetic field is introduced to collect size, shape, and phase controlled nanocrystals.

Cobalt and cobalt oxide nanocrystals were processed by chemical decomposition of $Co_2(CO)_8$ in toluene [23–25]. To disperse the freshly processed nanocrystals, sodium bis(2-ethylhexyl) sulfosuccinate [$C_{20}H_{37}O_2SNa$, in short, Na(AOT)] was added as a surface active agent, forming an ordered monolayer passivation (called the thiolate) over the nanocrystal surface. The thiolate serves not only as the protection layer for the particles to avoid direct contact between the particles with a consequence of collapsing but the interparticle bonding. 100 mg of $Co_2(CO)_8$ and 50 mg of Na(AOT) were dispersed into 25 ml of toluene at room temperature. The mixed solution was then ultrasonically dispersed and heated at 130 °C for 4 h in air. This temperature was chosen to enhance the crystallinity of the nanocrystals. By adjusting the wt. % ratio between the precursor and Na(AOT) from 1:1 to 5:1, the particle size was controlled to be smaller than 5 nm. Then the mixed solution was diluted to 1:4 by adding toluene. The as-prepared solution contained Co and CoO particles. Since Co particles are superparamagnetic when their sizes are smaller than 10 nm, while CoO is antiferromagnetic, a small magnetic field, generated by a horseshoe permanent magnet, was applied in the vertical direction (with the *N* pole at the top) so that the Co nanoparticles floated to the top surface of the liquid under the driving force of the magnetic field, forming aggregates, while the CoO particles were left in the solution. Relying on gravity force, the smaller size particles were suspended in the liquid, while the larger ones sank to the bottom. By picking the particles suspended at different depths of the solution after 24 h in the magnetic field, the size and phase selected nanoparticles were obtained. This magnetic field separation technique was very useful in this type of experiment, and the phase selected particles were highly monodispersive and pure. The structure of the nanocrystals was determined using transmission electron microscopy (TEM). For TEM observations, a drop of solution was deposited on an ultrathin carbon film supported by a copper grid. The TEM experiments were performed at 200 kV using a Hitachi HF-2000 TEM equipped with a field emission source, and at 400 kV using a JEOL 4000EX high-resolution TEM.

The particles reported here are in the size range of 4–5 nm; thus, the particle contrast is rather weak in conventional bright-field (BF) TEM images due to

 0031-9007/97/79(13)/2570(4)$10.00

the presence of carbon support and the thiolate layer. Figure 1(a) is a bright-field TEM image of the synthesized CoO nanocrystals, displaying ordered assembling with translational symmetry. It is amazing that almost all of the nanocrystals have the same size, and many particles show a triangular projected shape. The low-angle electron diffraction pattern gives the symmetry of the nanocrystal packing, and it is indexed as the $[110]_s$ orientation of a face-centered cubic structure, where the subscript s indicates the Miller index for the NCS. This pattern is a unique feature for eliminating the possibility of other types of packing, such as bcc or hcp. Using the high-angle diffraction rings from the CoO core as an absolute calibration, the lattice constant of the NCS is determined to be $a_s = 12 \pm 0.5$ nm, based on the low-angle diffraction spots.

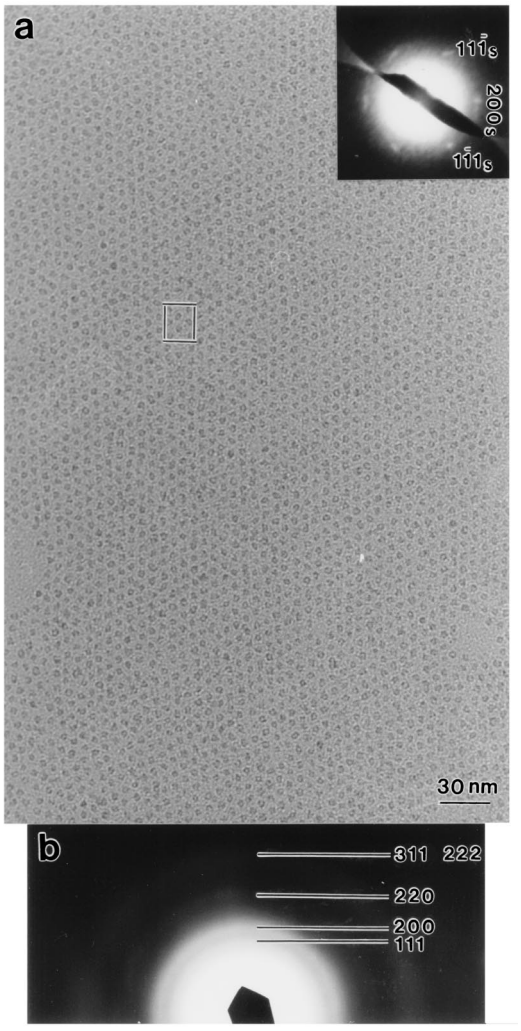

FIG. 1. (a) A bright-field TEM image of CoO nanocrystals, passivated with Na(AOT) and dispersed on carbon film, showing long-range ordered self-assembling. A low-angle diffraction pattern recorded from the NCS is shown in the inset, uniquely displaying $[110]_s$ fcc structure. The projected unit cell of fcc is indicated. (b) An electron diffraction pattern of a large area of the assembled nanocrystals, showing continuous diffraction rings. The central transmitted spot is blocked to ensure the exposure of the diffraction rings. The ring broadening due to the small size of the nanocrystals makes the {311} and {222} rings indistinguishable.

Dark-field (DF) TEM imaging has shown its potential in defining the multilayer stacking. DF-TEM imaging is formed by selecting the electrons scattered into an angular range defined by the position and size of the objective aperture. The low magnification DF-TEM image [Fig. 2(a)] clearly shows the regions with monolayer (at the sides) and multilayer (at the center) stacking based on the image contrast and local intensity. The long-range translational order is clearly evident. The nonuniform contrast of each individual particle in Fig. 2(b) is related to the particle's orientations. A Fourier analysis of the image has shown the $[110]_s$ projected face-centered cubic lattice of the NCS, although there are some distortions due to the particle shape, which will be discussed later.

The core crystal structure of the synthesized nanocrystals is determined by energy dispersive x-ray spectroscopy (EDS), electron diffraction, and electron energy-loss spectroscopy (EELS). The EDS spectrum [Fig. 3(a)] shows the presence of oxygen and cobalt; carbon comes from the thiolate passivation layer and the carbon support

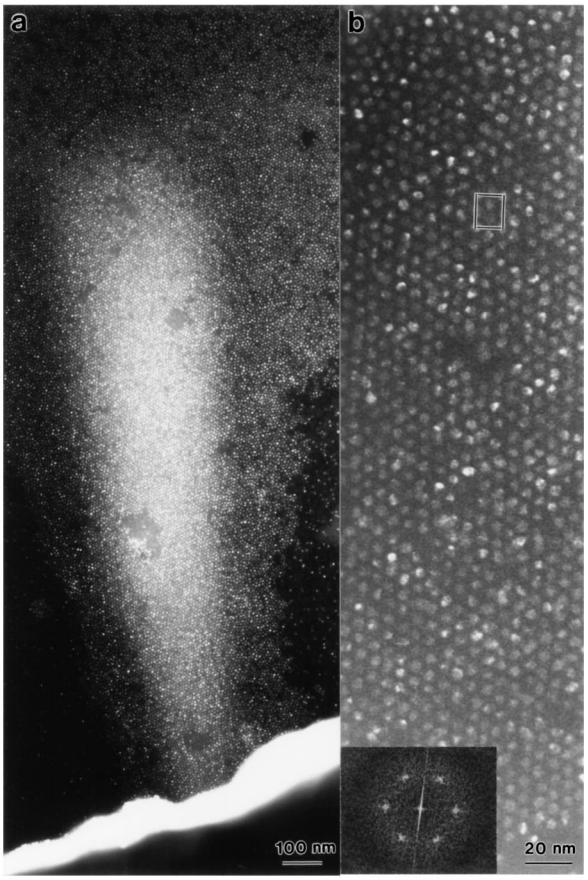

FIG. 2. (a) Dark-field TEM image of monolayer and multilayer NCS's, recorded at 400 kV by selecting a small portion of the {311} and {222} reflections. The projected unit cell of fcc is indicated. Inset: A Fourier transform of the image is given to show the ordered structure. (b) An enlargement of the image to show the nonuniform contrast across each particle, as will be used for defining the crystal shape.

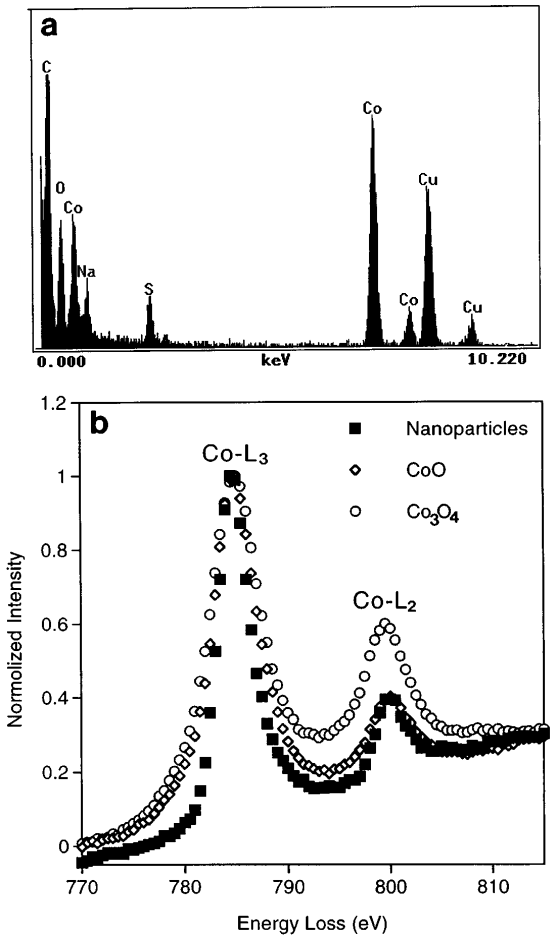

FIG. 3. (a) An EDS spectrum recorded from a self-assembled CoO NCS, exhibiting the fundamental elements present in the specimen. (b) A comparison of EELS spectra of Co-$L_{2,3}$ ionization edges acquired from Co_3O_4 and CoO standard specimens and the synthesized nanocrystals, proving that the valence state of Co is 2+ in the nanocrystals. The full width at half-maximum of the white lines for the Co_3O_4 and CoO standards is wider than that for the nanocrystals, possibly due to size effect.

film, Na and S are contained in Na(AOT), and Cu comes from the copper grid for supporting the carbon film. Quantitative analysis shows the ratio of O:Co ≈ 2, where the excess oxygen is contributed by Na(AOT) and the surface adsorbed oxygen on the carbon film. To determine the atomic structure of the nanocrystals, an electron diffraction pattern was recorded [Fig. 1(b)], where the observed ring pattern can be indexed as the NaCl-type structure. The diffraction intensity can be qualitatively understood based on kinematical scattering theory. Since CoO has the NaCl-type crystal structure, the diffraction intensity $I_{(hkl)} = 16(f_{\mathrm{Co}} - f_{\mathrm{O}})^2$ if the Miller index (h, k, l) are all odd, $I_{(hkl)} = 16(f_{\mathrm{Co}} + f_{\mathrm{O}})^2$ if (h, k, l) are all even, and $I_{(hkl)} = 0$ if (h, k, l) are mixed, where f_{Co} and f_{O} are the electron scattering factors of Co and O, respectively. Thus, the intensity of the {200} reflection is significantly stronger than that of {111}. Therefore, the crystal structure is identified as CoO, in agreement with the result expected from the magnetic field driven phase separation technique described above.

To confirm that the synthesized nanocrystals are CoO, EELS is used to measure the valence state of Co. In EELS, the L ionization edges of transition-metal and rare-earth compounds usually display sharp peaks at the near edge region, which are known as *white lines*. For transition metals with unoccupied 3d states, the transition of a 2p state electron to the 3d levels leads to the formation of white lines observed experimentally. The L_3 and L_2 lines are the transitions of $2p^{3/2} \rightarrow 3d^{3/2}3d^{5/2}$ and $2p^{1/2} \rightarrow 3d^{3/2}$, respectively, and their intensities are related to the unoccupied states in the 3d bands [26]. Figure 3(b) shows a comparison of the spectra acquired from Co_3O_4 and CoO standard specimens and the synthesized nanocrystals. The relative intensity of the Co-L_2 to Co-L_3 for the nanocrystals is almost identical to that for CoO standards, while the Co-L_2 line of Co_3O_4 is significantly higher, indicating that the Co valence in the nanocrystals is 2+; thus, the crystal structure is confirmed to be CoO.

The particle shape is revealed by the monolayer NCS owing to the absence of the overlapping effect in the projected crystal shape [Fig. 4(a)]. More than 75% of the nanocrystals have clearly shown the triangle projected shape. The size of the monolayer assembling can be as large as 3 μm, while the multilayer assembling is 1–1.5 μm. There are two possible geometrical configurations that are likely to give the projected triangular shapes in the nanocrystal system. One is a tetrahedron bounded by four {111} facets and the other is a (111) based platelet structure. If the latter was the structure seen here, the contrast of the nanocrystals in the dark-field image would be uniform because of the uniform thickness of the nanocrystal. In contrast, the experimental DF-TEM image shown in Fig. 2(b) clearly indicates that the contrast across each nanocrystal is nonuniform; rather there is a white dot in the image of each nanocrystal, suggesting that the nanocrystals have a tetrahedral shape, and the white dot corresponds to the projected position of the vertical apex of the tetrahedron. The nanocrystal size is measured in reference to the edge length, and the result gives 4.4 ± 0.2 nm. The average number of Co atoms in each nanocrystal is calculated to be $\sim$520 if the atom density in the particle is the same as in the bulk. The translation symmetry is preserved in the NCS's while the orientational order may only be short range. This is different from the fcc packing of Ag nanocrystals with truncated octahedron shape [15], in which both translational and orientational ordering are preserved for long range simply because of a higher-degree symmetry of the nanocrystal shape.

To further confirm the tetrahedral shape of the nanocrystals, high-resolution TEM (HRTEM) images were recorded from the nanocrystals [Fig. 4(b)], where the triangle projected shape of the nanocrystal is identified, although the image contrast is poor owing to

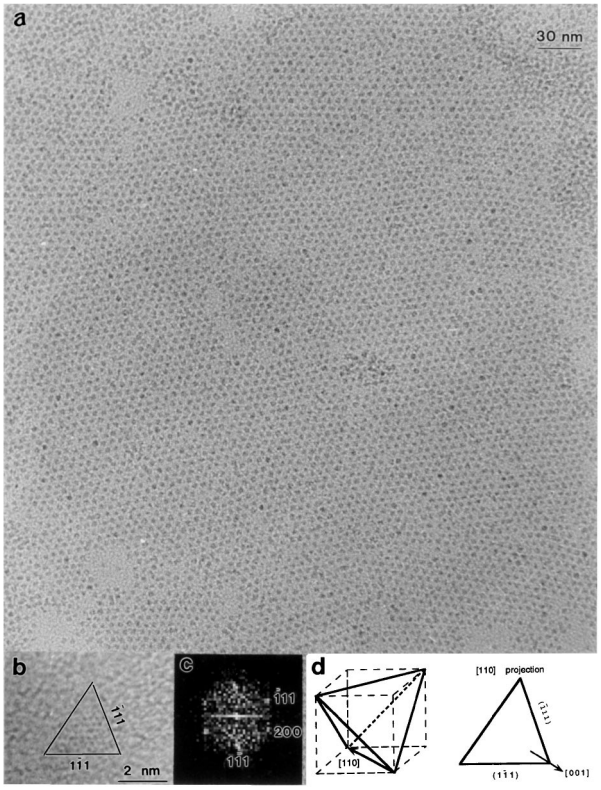

FIG. 4. (a) Bright-field TEM image of self-assembled monolayer CoO nanocrystals showing the dominant tetrahedral shape. (b) A high-resolution TEM image of a typical tetrahedral CoO nanocrystal oriented along [110], showing two edge-on {111} facets. (c) A Fourier transform of the image shown in (b) indicating the [110] orientation of the crystal and the face-centered cubic crystal structure (e.g., NaCl type). (d) Schematic models showing the 3D shape of the {111} enclosed tetrahedral nanocrystal and its [110] projection in correspondence to the image shown in (b).

the strong effect from the surface passivation layer, the carbon substrate, and the least density of the projected atoms at the edge of the nanocrystal due to the tetrahedral shape [Fig. 4(d)] as well as the weak scattering power of the O and Co atoms. A Fourier transform of the HRTEM image of the nanocrystal is given in Fig. 4(c), indicating that the nanocrystal is oriented along [110] and the projected cation columns show a darker spot contrast. A tetrahedron is formed by four {111} facets [Fig. 4(d)], and two of them are imaged edge on if the incident beam direction is [110] (Ref. [27]). The experimental image shown in Fig. 4(b) displays the $(\bar{1}11)$ and $(1\bar{1}1)$ facets, just as expected from the model.

In conclusion, tetrahedral nanocrystals of CoO, with edge lengths of 4.4 ± 0.2 nm, have been synthesized at high purity and monodispersity. The size, shape, and phase selections of the nanocrystals were performed using a novel magnetic field separation technique. These nanocrystals behave like molecules, forming face-centered cubic, self-assembled CoO nanocrystal superlattices.

This work was supported in part by NSF Grant No. DMR-9632823.

*To whom all correspondence should be addressed.
Electronic address: zhong.wang@mse.gatech.edu

[1] D. J. Wales, Science **271**, 925 (1996); all the review articles in the Feb. 16 issue of Science (1996).
[2] M. A. Kastner, Phys. Today **46**, No. 1, 24 (1993).
[3] L. N. Lewis, Chem. Rev. **93**, 2693 (1993).
[4] R. Freer, *Nanoceramics* (Institute of Materials, London, 1993).
[5] D. D. Awschalom and D. P. DiVincenzo, Phys. Today **48**, No. 4, 43 (1995); J. Shi, S. Gider, K. Babcock, and D. D. Awschalom, Science **271**, 937 (1996).
[6] J. F. Smyth, Science **258**, 414 (1992).
[7] P. V. Braun, P. Osenar, and S. I. Stupp, Nature (London) **380**, 325 (1996).
[8] H. Weller, Angew. Chem. **35**, 1079 (1996).
[9] T. S. Ahmadi, Z. L. Wang, T. C. Green, A. Henglein, and M. A. El-Sayed, Science **28**, 1924 (1996).
[10] W. D. Luedtke and U. Landman, J. Phys. Chem. **100**, 13 323 (1996).
[11] R. L. Whetten, J. T. Khoury, M. M. Alvarez, S. Murthy, I. Vezmar, Z. L. Wang, C. C. Cleveland, W. D. Luedtke, and U. Landman, Adv. Mater. **8**, 428 (1996).
[12] J. Dorogi, J. Gomez, R. Osifchin, R. P. Andres, and R. Refenberger, Phys. Rev. B **52**, 9071 (1995).
[13] D. V. Leff, P. C. Ohara, J. R. Heath, and W. M. Gelbart, J. Phys. Chem. **99**, 7036 (1995).
[14] R. P. Andres, T. Bein, M. Dorogi, S. Feng, J. I. Henderson, C. P. Kubiak, W. Mahoney, R. G. Osifchin, and R. Reifenberger, Science **273**, 1690 (1996).
[15] S. A. Harfenist, Z. L. Wang, M. M. Alvarez, I. Vezmar, and R. L. Whetten, J. Phys. Chem. **100**, 13 904 (1996); S. A. Harfenist, Z. L. Wang, M. M. Alvarez, I. Vezmar, and R. L. Whetten, Adv. Mater. (to be published).
[16] J. R. Heath, C. M. Knobler, and D. V. Leff, J. Phys. Chem. B **101**, 189 (1997).
[17] C. B. Murray, C. R. Kagan, and M. G. Bawendi, Science **270**, 1335 (1995), and references therein.
[18] L. Brus, Appl. Phys. A **53**, 465 (1991).
[19] A. P. Alivisatos, Science **271**, 933 (1996), and references therein.
[20] M. D. Bentzon, J. Van Wonterghem, S. Mørup, A. Thölen, and C. J. W. Koch, Philos. Mag. B **60**, 169 (1989).
[21] L. Motte, F. Billoudet, E. Lacaze, and M.-P. Pileni, Adv. Mater. **8**, 1018 (1996).
[22] S. I. Stupp, V. LeBonheur, K. Walker, L. S. Li, K. E. Huggins, M. Kerser, and A. Amstutz, Science **276**, 384 (1997).
[23] J. R. Thomas, J. Appl. Phys. **37**, 2914 (1966).
[24] J. P. Chen, C. M. Sorensen, K. J. Klabunde, and G. C. Hadjipanayis, Phys. Rev. B **51**, 11 527 (1995).
[25] E. Papiper, P. Horny, H. Balard, R. Anthore, C. Petipas, and A. Martinet, J. Colloid Interface Sci. **94**, 207 (1983).
[26] D. H. Pearson, C. C. Ahn, and B. Fultz, Phys. Rev. B **47**, 8471 (1993); H. Kurata and C. Colliex, Phys. Rev. B **48**, 2102 (1993); Z. L. Wang, J. S. Yin, Y. D. Jiang, and J. Zhang, Appl. Phys. Lett. **70**, 3362 (1997); Z. L. Wang and J. S. Yin, Philos. Mag. B (to be published).
[27] HRTEM studies of tetrahedral nanocrystals have been described in detail by A. P. Alivisatos, J. Phys. Chem. **100**, 13 226 (1996); Z. L. Wang, T. S. Ahmadi, and M. A. El-Sayed, Surf. Sci. **380**, 302 (1997).